



Performance of the Transition Radiation Detector of the MACRO experiment

The MACRO collaboration *
presented by M. N. Mazziotta

A transition radiation detector (TRD) consisting of three identical modules each of 12 m² area, has been developed and installed on the MACRO detector at the Gran Sasso National Laboratory. The modular structure, based on single proportional tubes and polyethylene foam radiators, allows to cover a large area. The TRD measures the residual energies (up to 1 TeV) of penetrating muons at the MACRO depth. Calibrations from prototypes operated in a test beam at the CERN P.S. are quoted. We present the preliminary data from the first TRD module, collected in a period of about one year.

1. INTRODUCTION

High energy muons produced by primary cosmic rays interacting with atmospheric nuclei have been investigated to extract information about the primary component and its interaction cross section.

The muon energy spectrum deep underground can be derived from the surface muon spectrum and from calculations of energy losses, using assumptions on the interaction cross sections of high energy muons in the rock.

A direct measurement of this spectrum therefore can give information on the interaction mechanisms of muons in the rock, and can be used to confirm the surface muon spectrum and the “all-nucleon” primary cosmic ray spectrum.

An attempt was made ten years ago [1] to measure the residual energy spectrum of cosmic ray muons reaching the Mont Blanc underground laboratory. In that case a small transition radiation detector (TRD) was installed on top of the NUSEX detector [2].

In order to increase the MACRO detector capabilities with a device able to measure the residual muon energy we designed and built a large area TRD. The TRD allows the energy measurement of each muon up to the TeV region, although with modest resolution. This measurement may open a wide range

of experimental opportunities for cosmic ray physics in underground laboratories. With this technique, the residual energy of downgoing, and eventually of neutrino induced upgoing muons, is directly measured.

2. THE MACRO TRD

2.1. Properties of transition radiation

Transition radiation detectors (TRDs) are presently of interest for fast particle identification both in experiments at the new generation of accelerators [3] and in cosmic ray physics [4,5]. TRDs have also been proposed and developed to measure the energy of cosmic ray muons in the TeV region [1,2,6]. Due to the characteristic dependence (in a limited energy range) of transition radiation on the Lorentz factor γ of the incident particle, it is possible to evaluate its energy $E = m_o \gamma c^2$ in the same energy range if the rest mass m_o is known, or if the particle has been identified, as is the case of muons reaching an underground laboratory.

Transition radiation (TR) is emitted in the X-ray region whenever an ultrarelativistic charged particle crosses the boundary of two materials with different dielectric properties [7]. For each interface the emission probability for an X-ray photon is of the order of $\alpha = 1/137$ (fine structure constant). Radiators consisting of some hundreds of foils regularly spaced are used to enhance X-ray production; a few photons are

*For the complete list of authors see the paper by N. Giglietto in these proceedings

produced allowing a reliable tagging of the fast particle.

The multilayer radiator introduces physical constraints for the radiation yield, due to the so called “interference effects”. The radiation emission practically starts at a Lorentz factor $\gamma_{th} = 2.5\omega_p d_1$, where ω_p is the plasma frequency (in eV units) of the foil material, and d_1 is its thickness in microns [8]. At higher γ the radiation energy increases up to a saturation value $\gamma_{sat} \sim 0.6\gamma_{th}(d_2/d_1)^{1/2}$ [8], where d_2 is the distance of the gap between the foils. Similar behaviours have been observed for irregular radiators such as carbon compound foam layers or fiber mats [4,9], where the role of the thin foil is played by the cell wall and by the fiber element, and the gap by the cell pore and by the fiber spacing.

The multilayer plastic are produced at low cost; their densities (and hence the cell or fiber sizes and spacings) can be selected in order to produce increasing transition radiation in the γ -range $10^3 - 10^4$; for muons this corresponds to energies of 100 GeV–1 TeV. We tested a large variety of materials trying to obtain the maximum photon yield with the minimum radiator thickness, while maintaining at same time the widest $\gamma_{th} - \gamma_{sat}$ range [10].

Gaseous chambers working in the proportional region are generally preferred to solid state or scintillation counters to detect transition radiation. In fact, the radiating particle, if not deflected by magnetic fields, releases its ionization energy in the same region as the X-ray photons, introducing a background signal that can be reduced if a gaseous detector is used. The gas must provide efficient conversion of the TR photons; therefore high Z gases are generally used, such as argon, krypton or xenon.

Two methods are used for the chamber readout:

- the “charge measurement” method, where the signal collected from the chamber wire is amplified and then charge analyzed by ADCs [11];
- the “cluster counting” method, where the wire signal is sharply differentiated in order to discriminate δ -rays background

from the clusters of ionization from X-ray photoelectrons producing pulses (hits) exceeding a threshold amplitude [12].

In these methods a cut on the analyzed charge and on the number of counts discriminates radiating particles from slower nonradiating ones.

Multiple module TRDs, with optimized gas layer thicknesses, are employed to improve background rejection; in these cases a reduced chamber gap limits the particle ionizing energy losses, while those X-rays escaping detection may be converted in the downstream chambers.

2.2. Detector layout

We have built three TRD modules of 36 m^2 total area for the MACRO experiment [13] at the Gran Sasso Laboratory (LNGS). The lab is located at an average depth of 3700 hg/cm^2 , with a minimum depth of 3150 hg/cm^2 . At these depths the residual energy differential distribution of the downgoing muon is estimated to be nearly flat up to 100 GeV and it falls rapidly in the TeV region; the mean value is of a few hundred GeV. The TRD has been designed to explore the muon energy range of 100 GeV – 1 TeV. Below 100 GeV there is no TR emission; from 100 GeV to 1 TeV the detector has a smoothly increasing response versus γ . For energies greater than 1 TeV, where the ordinary muon flux is estimated to be approximately 5% of the total, the TR signal is saturated.

The multiple muon events collected by the MACRO detector are of the order of 5–6 % of the total; the average separation between the muons is a few meters [14]. Thus a large area TRD is necessary to study the multimMuon energy spectrum.

The TRD consists of proportional tubes, 6 meters long, with a square cross section of $6 \times 6 \text{ cm}^2$; the tubes have thin polystyrene walls ($\leq 1 \text{ mm}$). These counters are laid close together between radiator layers, to form a large multiple layer TRD, with reduced inefficient zones.

The chosen cross section is a compromise between the need to have a high efficiency to convert the TR photons in the argon-based gas mixture, keeping at the same time the ionization energy release of the muon at a relatively low

level. The design parameters were based on Monte Carlo calculations [15] and on subsequent tests in a pion/electron beam at energies of 1-5 GeV (corresponding to a γ -range of about $10^3 - 10^4$).

The number of TRD layers is ten; this leads to a reduced number of channels and to a detector size which can be accommodated in the available height in the upper part of the MACRO apparatus (about two meters). The radiator thickness was limited for the same reason to 10 cm.

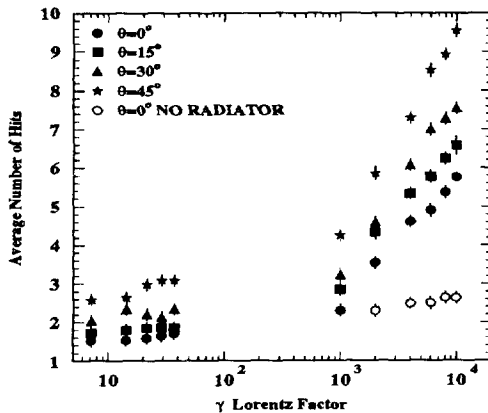


Figure 1. Average total number of hits for various values of the γ factor : dots: 0° incident beam angle; open circles: 0° beam angle without radiator; squares: 15° beam angle; triangle: 30° beam angle; stars: 45° beam angle.

As radiator material we selected Ethafoam 220 (about 35 g/l density) that exhibits cells of approximately 0.9 mm diameter and 35 μ m wall thickness, thus ensuring a relatively wide $\gamma_{th} - \gamma_{sat}$ range for the γ -factor. The TR spectra from Ethafoam of equivalent density have already been measured by many authors [4,17] and match properly with the transmission characteristics of the tube wall.

Each TRD module has an active volume of $6 \times 1.92 \times 1.7 \text{ m}^3$ and contains 32 tubes per layer, interleaved by the foam radiators. The bottom tube layer is placed on the top of an eleventh radiator: in this way the detector is symmetric with respect to downgoing and

upgoing muons, thus offering the additional opportunity to measure the energy of neutrino induced muons penetrating into the laboratory from the floor.

With a reduced scale prototype exposed to a pion/electron test beam we developed and used a simple and efficient read-out electronics. In two recent papers [10,18] we have analyzed both the behaviour of the TR energy versus γ (charge analysis and cluster counting). We found that the second method gives results consistent with that of the TR energy, as reported by other authors [19]. After accurate calibration runs in the test beam, we have equipped the TRD with cluster counting electronics, which proved to be more reliable and less expensive for our experiment.

The total cluster count (total number of hits) released in the TRD can be fit by a Poisson distribution. The γ resolution (and consequently the muon energy resolution) is modest, since the average of the Poisson distributions at different energies are at best of the order of ten hits.

In Fig. 1 the TRD response, namely the average number of hits at various γ , and various beam crossing angles is shown. For graphic reasons, the mean number of hits obtained with electrons without radiators are indicated only for 0° incidence.

Fig. 2 shows the TRD display of a typical event triggered by the MACRO detector: we observe a muon crossing the TRD from the top. The trigger is provided by the MACRO muon streamer trigger [16].

3. DATA SELECTION

In this analysis we have considered the data collected from April 1994 to January 1995 by the first TRD module.

Since the TRD calibration was performed for particles crossing the ten layers and at zenith angles below 45° , in the analysis only single muons fulfilling these constraints have been included [20].

The muon energy is evaluated by counting the number of TRD hits (in the view perpendicular to the anode wires) along the straight line fitted to the track reconstructed by the MACRO detector.

In Fig. 3 we report the distribution of the number of hits in the track for these muons.

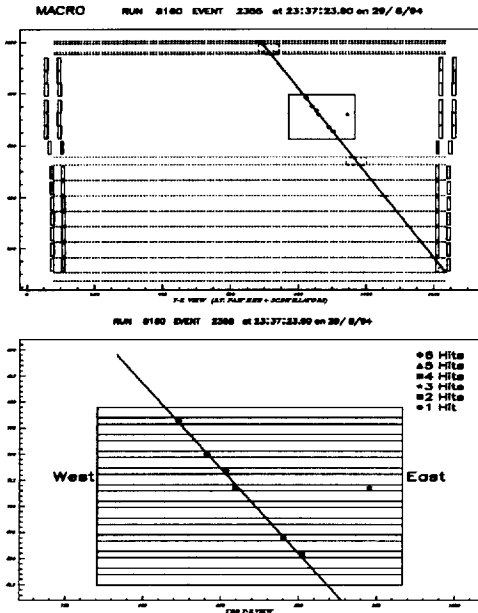


Figure 2. On-line display of a typical single muon crossing MACRO and the TRD (upper part). In the lower part an enlarged view of the TRD is shown.

4. MUON ENERGY SPECTRUM

In order to evaluate the local muon energy spectrum, we must take into account the TRD response function, that induces some distortion of the “true” muon spectrum distribution. The “true” distribution can be extracted from the measured one by an unfolding procedure that yields good results only if the response of the detector is correctly understood.

We have adopted an unfolding technique, developed according to Bayes’ theorem, following the prescriptions of [21,22]. Usually the unfolding methods require that the independent variable (the energy) is limited inside a finite interval. When it is practically boundless, as for the cosmic ray energy spectrum, the method cannot be

automatically applied. In our case however this problem can be overcome since the detector response is flat outside the 100 GeV–1 TeV energy interval; thus the number of hits related to the energy is effectively “bounded”.

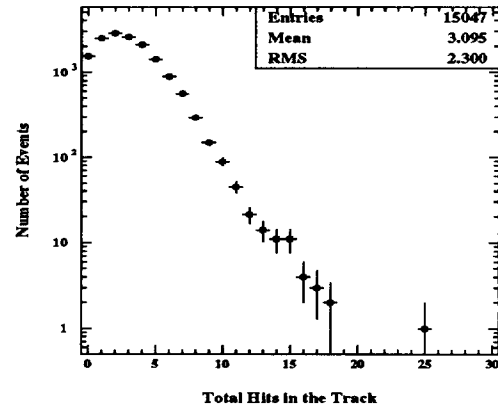


Figure 3. Hit distribution for single muon tracks crossing the TRD. Only statistical errors are shown.

4.1. Detector simulation

The distributions of the hits collected along a muon track by the TRD at a given zenith angle, $N(k, \theta)$, can be related to the residual energy distribution of muons, $N(E, \theta)$, by:

$$N(k, \theta) = \sum_{j=1}^{n_E} p(k | E_j, \theta) N(E_j, \theta) \quad (1)$$

where the detector response function, $p(k | E_j, \theta)$, represents the probability to observe k hits for a track of a given energy E_j and at a given angle θ .

The response function must contain both the detector acceptance and the event reconstruction efficiency. We have derived the response function simulating the MACRO behaviour using GEANT [23], including the trigger efficiency simulation. The simulation of the TRD was based on the test beam calibration data, taking also into account the proportional tubes inefficiency effects.

The detector response function was computed assuming a muon spectrum flat versus energy, θ and ϕ ; the response was calculated as the ratio of

the number of events producing k hits at a given energy and angle θ , divided by the total number of the events in the same energy and θ bins [20].

4.2. Experimental data distributions

The unfolding procedure described above was applied to the TRD experimental data, starting with initial probabilities assigned to the unfolded distribution [21], according to a local energy spectrum of muons at 4000 hg/cm^2 with a spectral index fixed of 3.7 given by [24]:

$$p_o(E) \sim e^{-\beta h(\alpha-1)}(E + \epsilon(1 - e^{-\beta h}))^{-\alpha} \quad (2)$$

The parameters are: $h = 4 \text{ km w. e.}$, $\alpha = 3.7$, $\beta = 0.383 \text{ (km w. e.)}^{-1}$ and $\epsilon = 0.618 \text{ TeV}$ [20].

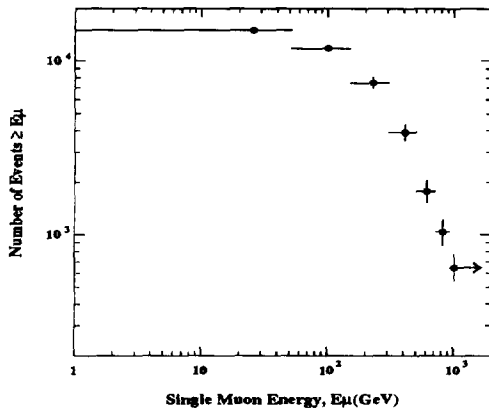


Figure 4. Integral energy distribution of single muons in the TRD. The last bin to the right is relative to energies larger than 930 GeV (the saturated region of the TRD). Horizontal bars indicate the bin width, while vertical bars indicate the total error (inclusive of statistical and systematic uncertainties).

Because the TRD behaviour shows a saturated region (for $E_\mu \geq 930 \text{ GeV}$), then in that range only the number of events can be evaluated, while below 930 GeV we can reconstruct the energy distribution and we can compute the average value truncated to 930 GeV.

Fig. 4 shows the integral muon integral spectrum; Fig. 5 shows the average muon energy truncated to 930 GeV, as a function of the

rock depth. The error bars include statistical and systematic uncertainties. The systematic uncertainties are due to the calibration data (estimated to be $\pm 1 \%$), and to the efficiency corrections (estimated to be $\pm 2 \%$). The systematic uncertainties have been propagated by changing the calibration input data and the correction factors in the unfolding procedure.

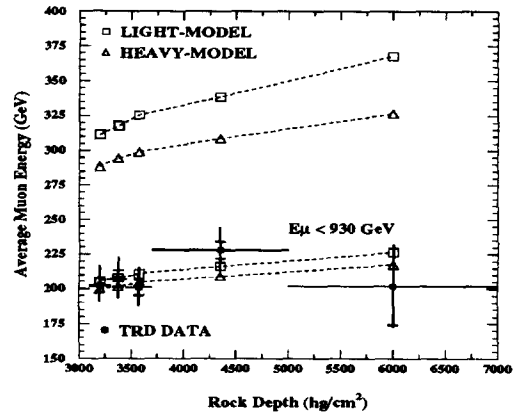


Figure 5. The lower part of the picture shows the average single muon energy, truncated to 930 GeV, versus the standard rock depth. The experimental data are shown together with the predictions of two primary composition models. In the upper part of the figure, the same distributions, with the same symbols, for the not-truncated case are shown. The extensions of the statistical error bars represent the estimates of systematic uncertainties. The dotted lines are drawn to guide the eye.

5. DISCUSSION

The muon spectrum is slightly sensitive to the all-nucleon spectrum of primary cosmic rays and to the energy losses in the rock. We have compared our results to the predictions from two extreme hypotheses on the primary spectra [25], namely the “Light” [26] and the “Heavy” [27] compositions. The interaction of the cosmic rays in the atmosphere was simulated with the HEMAS code [28]. The produced muons at surface were then propagated through the rock,

with the muon energy loss in the rock evaluated according to the prescriptions of Lipari and Stanev [24]. The rock thickness was calculated at each θ and ϕ from the Gran Sasso map [29]. We used the correction procedure described in [30] for the conversion to standard rock.

Fig. 5 shows the average muon energies relative to the two predictions, truncated to 930 GeV, together with experimental data (lower part of the figure), the non truncated analysis is shown in the upper part. Our experimental data, after corrections for the propagation of the muons through the Gran Sasso rock, are consistent, within the errors, with the above predictions. The present precisions do not allow to distinguish between the above models.

6. CONCLUSIONS

We have measured directly the residual energy of cosmic ray muons crossing the MACRO detector at the Gran Sasso underground laboratory, using a TRD which took data since April 1994. The average energy, truncated to about 1 TeV, is about 200 GeV in the depth range 3000–7000 hg/cm^2 .

In spite of the TRD resolution, the muon energy measurement in underground experiment can give useful information about the energy losses of muons in the rock and about the surface muon spectrum.

REFERENCES

1. M. Calicchio et al., Phys. Lett. B 193 (1987) 131
2. M. Castellano et al., Nucl. Instr. and Meth. A 256 (1987) 38
3. B. Dolgoshein, Nucl. Instr. and Meth. A 326 (1993) 434
4. T.A. Prince et al., Nucl. Instr. and Meth. 123 (1975) 231
5. E. Barbarito et al. Nucl. Instr. and Meth. A 357 (1995) 588
6. K.G. Antonian et al., XXIII Conference on Cosmic Ray Physics, H.E.7.1 (1987)
7. G.M. Garibian, Sov. Phys. JETP 6 (1958) 1079
8. X. Artru et al., Phys. Rev. D 12 (1975) 1289
9. A. Bungener et al., Nucl. Instr. and Meth. 214 (1983) 261
10. R. Bellotti et al., Nucl. Instr. and Meth. A 305 (1991) 192
11. J. Fischer et al., Nucl. Instr. and Meth. 127 (1975) 525
12. C.W. Fabjan et al., Nucl. Instr. and Meth. 185 (1981) 119
13. The MACRO Collaboration, S.P. Ahlen et al., Nucl. Instr. and Meth. A 324 (1993) 337
14. The MACRO Collaboration, S.P. Ahlen et al., Phys. Rev. D 46 (1992) 4836
15. M. Castellano et al., Comp. Phys. Comm. 61 (1990) 395
16. The MACRO Collaboration, M. Ambrosio et al., LNGS 95/12 (1995)
17. M.L. Cherry, Phys. Rev. D 17 (1978) 2245
18. E. Barbarito et al. Nucl. Instr. and Meth. A 365 (1995) 214
19. A. Denissov et al., Preprint Fermilab Conf. 84/134E (1984)
20. The MACRO Collaboration, M. Ambrosio et al., MACRO/PUB 96/6 (1996)
21. G. D'Agostini, Nucl. Instr. and Meth., A 362 (1995) 487
22. M.N. Mazziotta, LNGS 95/52, (1995)
23. R. Brun et al., CERN Public. DD/EE/84-1 (1992)
24. P. Lipari and T. Stanev, Phys. Rev. D 44 (1991), 3543
25. The MACRO Collaboration, M. Ambrosio et al., INFN/AE-96/29 (1996)
26. C. Fichtel and J. Linsley, Astrophys. J. 300 (1986) 474
27. J.A. Goodman et al., Phys. Rev. D 26, (1982) 1043
28. C. Forti et al., Phys. Rev. D 42 (1990) 3668
29. The MACRO Collaboration, M. Ambrosio et al., Phys. Rev. D 52 (1995) 3793
30. A.G. Wright, Proc. of 12th ICRC, Denver (USA), 3 (1973) 1709